HHS Public Access

Author manuscript

Lab Chip. Author manuscript; available in PMC 2022 September 28.

Published in final edited form as:

Lab Chip. ; 21(19): 3667–3674. doi:10.1039/d1lc00465d.

Point of care whole blood microfluidics for detecting and managing thrombotic and bleeding risks

Scott L. Diamond, PhD[*], **Jason Rossi, PhD**

Institute for Medicine and Engineering, Department of Chemical and Biomolecular Engineering, 1024 Vagelos Research Laboratory, University of Pennsylvania, Philadelphia, PA 19104

Abstract

Point-of-care diagnostics of platelet and coagulation function present demanding challenges. Current clinical diagnostics often use centrifuged plasmas or platelets and frozen plasma standards, recombinant protein standards, or even venoms. Almost all commercialized tests of blood do not recreate the in vivo hemodynamics where platelets accumulate to high densities and thrombin is generated from a procoagulant surface. Despite numerous drugs that target platelets, insufficient coagulation, or excess coagulation, POC blood testing is essentially limited to viscoelastic methods that provide a clotting time, clot strength, and clot lysis, while used mostly in trauma centers with specialized capabilities. Microfluidics now allows small volumes of whole blood (<1 mL) to be tested under venous or arterial shear rates with multi-color readouts to follow platelet function, thrombin generation, fibrin production, and clot stability. Injection molded chips containing pre-patterned fibrillar collagen and lipidated tissue factor can be stored dry for 6 months at 4C, thus allowing rapid blood testing on single-use disposable chips. Using only a small imaging microscope and micropump, these microfluidic devices can detect platelet inhibitors, direct oral anticoagulants (DOACs) and their reversal agents. POC microfluidics are ideal for neonatal surgical applications that involve small blood samples, rapid DOAC testing in stroke or bleeding or emergency surgery situations with patients presenting high risk cofactors for either bleeding or thrombosis.

Graphical Abstract

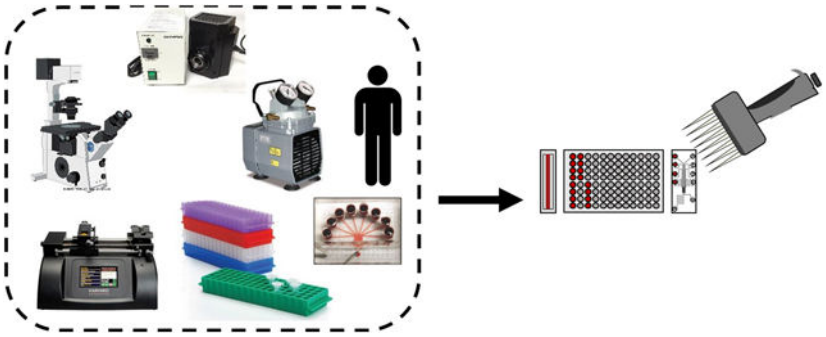

The development of microfluidic techniques for study of hemostatic processes has enabled research into different disease states, drug actions, biophysical phenomena, and elucidation of

[*]Corresponding author. Tel: 215-573-5702, sld@seas.upenn.edu.

coagulation reaction networks. The continuing refinement of microfluidic techniques from “chip in a lab” to true point-of-care capable techniques will enable a new generation of clinical testing and research devices.

Keywords

hemodynamics; platetets; thrombin; fibrin; anticoagulation

INTRODUCTION

The hospital coagulation laboratory deploys skilled personnel, centrifuges, manual and robotic liquid handlers, various readers, and complex reagent supply chains including venoms, antibodies, recombinant calibration proteins, and plasma standards. In this setting, pre-analytical variability such as phlebotomy, delay times, and anticoagulation has been managed for decades by international standardization committees in place since the use of rabbit brain thromboplastin. This infrastructure exists because measuring thrombotic and bleeding risks drives decisions in diverse situations: cardiovascular disease, hemophilia, post-operative bleeding, pregnancy and delivery, sepsis, trauma, and cancer. This is the known world of blood counts, plasma clotting times, platelet aggregometry, and more recently viscoelastic testing.

Because blood is flowing throughout the vasculature, biophysics and bioengineers have contributed their fluid mechanical expertise to help quantify molecular interactions, forces, and rates of blood clotting. The large parallel-plate flow chambers, capillary tubes, and Chandler loops used since the 1970s[1–3] set the stage for the advancement of microfluidic devices over the last 15 years.

Early microfluidic devices for analyzing blood clotting include the work from the Ismagilov lab[4] where fluorocarbon-encapsulated plugs of blood moved through a channel as thrombin and fibrin formation was imaged to yield an aPPT (activated partial thormboplastin time). In 2008, Neeves et al. developed a PDMS microfluidic device[5] for small blood samples (< 1 mL such as from mouse) where whole blood was perfused at venous or arterial shear rates to form clots on patterned collagen, revealing a role for PAR4 signaling in clot stability.

Microfluidics offers opportunities for point of care (POC) diagnostics by taking advantage of small whole blood samples, the liquidity of blood, controllable fluid dynamics to mimic physiology of venous or arterial blood function, multiplexing, and replicates. Even the extreme hemodynamics (10^4 to 10^5 s^{-1} wall shear rate) found in stenotic coronary arteries can be recreated with microfluidics[6–8]. In contrast, the low flow recirculation zones of vein valve thrombosis related to deep vein thrombosis can be recreated with microfluidics[9]. For lab on a chip devices, collagen, laminin, VWF, lipidated tissue factor (TF) for the extrinsic pathway initiation, and even kaolin (for contact activation of Factor XII) have all been coated or micropatterned on surfaces to initiate clotting[10–13]. However for POC, the technological challenges are numerous in the desire to avoid centrifugation, complicated reagent handling, manual pipetting, refrigerated or frozen components, and hours-long data turnaround. Importantly, no calibration standards exist for healthy living platelets. ***This***

review explores Lab-Chip configurations for monitoring: (1) fluid mechanics and clot composition, (2) drug responses under flow, and (3) point-of-care technologies for whole blood testing.

1) Fluid mechanics and clot composition

Blood clotting relies on the rapid response of platelets to vessel damage, typically fibrillar collagen activating platelet GPVI signaling that then triggers integrin activation ($\alpha_2\beta_1$ for collagen and $\alpha_{2b}\beta_3$ for fibrinogen and von Willebrand factor (VWF). Platelet dense granule release of ADP and cycloxygenase-dependent synthesis of thromboxane A2 (TXA_2) within a platelet deposit drives further clot growth. Under flow, dense platelet deposits provide a flow-sheltered, phosphatidylserine-rich procoagulant porous media in which the extrinsic coagulation cascade leads to thrombin generation and fibrin polymerization. The transport physics, platelet signaling dynamics, VWF mechanobiology, and systems biology of coagulation are well reviewed[14–16] and serve as the foundation for design of lab on a chip microfluidics[17]. In the body or on the chip, fluid motion is required to bring platelets in contact with each other. At the vessel-blood interface, flowing blood creates an RBC-depleted plasma layer enriched in platelets[18]. Therefore, whole blood testing of coagulation is central to microfluidics, allowing results that would not be observable with platelet rich plasma (PRP), plasma, or protein mixtures. Additionally, direct whole blood testing is faster and avoids dilutions, cell separations, or centrifugation.

Surface patterning: microspotting and micropatterning—Laboratories have used pin-tool delivery for spotting of mixtures of fibrillar collagen, VWF, laminin, etc. to explore platelet receptor signaling[19,20]. Pin-tools provide a dense array of 100 to 200 μm-diameter protein spots. These protein arrays are then mounted in a flow chamber. The combinatorial mixtures are well suited for pin-tooling to drive high dimensional functional phenotyping of the blood response to surface triggers[20]. Similarly, microfluidic patterning exploits surface binding to create dense lines of protein that are 250 micron to <10 microns in width[5,10,21]. The patterned glass slide substrates are then assembled as the final wall of the flow channels within the PDMS device.

Clot structure under flow—The first arriving platelets experience strong GPVI activation on collagen resulting in granule release and P-selectin display. Src family kinase inhibitors such as dasatinib strongly reduce this accumulation on collagen[22,23] and the exposure of phosphatidylserine (PS) by a minority of platelets[24]. Platelet deposition and activation continues on collagen/TF surfaces with a typical growth rate in clot height of about 60 micron over 10 minutes. The increase in channel height allows longer experiments and experimental designs where the perfusion liquid and perfusion flow rate can be acutely changed on a non-occlusive clot[25].

Structurally, clots formed by whole blood perfused over collagen contain a dense core of highly activated P-selectin positive platelets surrounded by a shell of less adherent and P-selectin negative platelets[26–29]. The core-shell morphology is observed in vivo in mouse arterioles[30] and venules, as well as larger vessels[31]. The mechanics of erosion of shell platelets was recently studied in a perfusion/shear switch experimental design[25]. In

addition to core/shell spatial variations of P-selectin, thrombin and fibrin are located in the clot core in close proximity to surface presented TF. Additionally, platelet contraction can pull on fibrin and collagen resulting not only in a more dense structure, but also the extrusion and sorting of PS+ platelets to the periphery of platelet deposits, a process reduced by the presence of fibrin[32]. Clot contraction force has been measured in a novel micropost-deformable sensor microfluidic device where 2–10 μN forces were detected for clots formed under flow[33].

Prior to thrombotic occlusion in vivo, shear rates can become extreme and drive VWF unfolding and aggregation into dense bundles that have been observed in animal models[34] and larger scale stenosis models[35,36]. Interestingly, recent analysis of hemorrhagic bleeding indicates pathologically high shear stresses at the wound exit[37]. At longer times when the channel is fully occluded, the clot sustains a significant pressure drop that drives a complex Darcy flow through cannuliculi of the clot, allowing neutrophils and red blood cells to move across the clot. Shear-induced NETosis (SINs) can be observed at pressure drops >70 mm-Hg/cm-clot. Similar to PS sorting, fibrin formation can reduce the formation of SINs[38]. Thus, fibrin mechanically stabilizes the clot to the procoagulant surface, reduces sorting, reduces NETosis, and binds a majority of thrombin produced inside the core region[39].

In terms of microfluidic design and operation, constant pressure drop flows best mimic the in vivo setting where an occlusion diverts flow. Constant flow rate experiments are similar to constant pressure drop experiments until ~75 % occlusion where upstream pressures and stenotic shear stresses become unphysiological. Constant flow rate experiments are technically easier to implement with a syringe pump and can mimic a constant pressure drop experiment if “flow diversion” pathway is present so the proximal side of the clot is not over-pressurized[40].

Additional microfluidic devices have been designed to recreate the pathological shear forces of coronary stenosis[41]. These devices exploit shear induced platelet activation and shear induced VWF unfolding to drive clot formation at the site of thrombosis. Recently, van Rooij et al.[42] deployed a constant pressure device to perfuse heparinized porcine whole blood and PRP through a channel whose height narrowed with different entrance lengths to control not just peak shear stress but also the spatial shear stress gradient entering the stenotic zone. In this work, a collagen coating was deployed as a trigger for platelet activation. In these configurations, occlusion occurs within 200 sec for whole blood over the range of 3000 to 12,000 s^{-1} initial wall shear rate.

2) Drug response under flow

Anticoagulation—Microfluidic testing of human whole blood can be conducted in the presence or absence of thrombin, depending on anticoagulation and composition of the triggering surface. While citrate is most common clinically, its reversal requires careful addition of calcium and factor XIIa can be generated by surfaces in citrated blood. For microfluidic tests of thrombin production, corn trypsin inhibitor (CTI) can be used at high doses (40–100 μg/mL) to prevent contact activation or at low dose (1–5 μg/mL) to allow activity of Factor XIIa or Factor XIa to be investigated[43]. High dose CTI prevents the generation of fragment 1.2 (F1.2) released by prothrombin conversion when whole blood is

perfused through a PDMS device primed with albumin buffer, but lacking a procoagulant surface[44].

Pharmacology of thrombosis and hemostasis—Numerous drugs, inhibitors, and proteins have been tested under microfluidic flow conditions. Certain drugs such as $P2Y_{12}$ inhibitors that reduce platelet signaling and integrin function are particularly potent at arterial shear forces that load platelet-platelet interactions[45]. Other drugs like apyrase that quench autocrinic ADP activation and aggregation in static PRP conditions are ineffective and potentially thrombogenic under flow[10]. This can be explained by the high density of platelets in deposits formed under flow that results in high concentrations of granule-released ADP and ATP, the latter converted to ADP by apyrase. In general, small molecule inhibitors are expected to equilibrate with receptors on the sub-second time scale and may present similar IC50s in microfluidic clotting and tube assays or aggregometry. In contrast, enzymes (apyrase) or antibodies may experience kinetic limitations or intrathrombus transport limitations of their efficacy and their IC50 may be shear dependent. Blood from hemophiliacs, trauma patients, and neonates can perform quite differently from that of average healthy donors.

Table 1 is a partial listing of pharmacological agents that target platelets or coagulation and their performance under microfluidic assay. Interpretation of mechanism of action or potency should always consider prevailing wall shear rate, anticoagulation protocol, the presence or absence of thrombin/fibrin generation, and (quite importantly) the traits of the blood donor. Blood from hemophiliacs, trauma patients, and neonates can perform quite differently from that of average apparently healthy donors.

3) Point-of-care technologies for whole blood testing

A point of care (POC) device for monitoring coagulation state typically requires a pre-assembled and ready to use microfluidic component (the chip) that contains on-chip reagents and a small instrument to control fluid motions and to read output signals. The chip may or may not necessarily be linked to a “cartridge or well plate” that facilitates macro-micro connections. The storage stability for reagents may require frozen, refrigerated, or ideally lyophilized reagents with at least 6-month room temperature storage, a challenging goal for the many diverse reagents used in coagulation testing.

Various commercialized POC whole blood technologies include: VerifyNow, Platelet Function Analyzer (PFA), and viscoelastic testing (TEG, ROTEM, and sonorheology). Only the PFA-100 incorporates flow as an intrinsic feature of the assay, with an ability to detect deficiencies in VWF and ADP function at high shear rates[55]. The PFA cartridge requires 0.8 mL of whole blood per run. Assays such as platelet aggregometry, PT, aPTT typically are not bedside[56]. Point of care implementations of PT/INR such as CoaguChek, and iSTAT products, utilize 10–40 μL of whole blood which is added to a chip/test strip containing thromboplastin reagent. The detection method varies, including optical, mechanical and electrical technologies. Typically, the usage of whole blood rather than plasma increases the variability associated with POC PT/INR tests, compared with their standard laboratory counterparts[57,58].

Several microfluidic devices for whole blood research have been developed over the last 10 years in academic laboratories, utilizing varied geometries and wetted materials for different purposes. Utilizing serpentine flow elements with stenoses regions to create pathophysiological shear, Jain et al.[59] developed a device for real time coagulation monitoring of porcine blood in extracorporeal circuits. Devices were coated with collagen as a platelet agonist, and significant deposition was observed in the post-stenosis regions of the device. Clot time was increased for human blood upon addition of aspirin/Plavix and abciximab. Vascularized flow channels have also been demonstrated by several groups. Jain et al. demonstrated a PDMS device with 6 independent straight channels (400 by 100 μm), coated with collagen and lined with HUVECs and then fixed via formaldehyde[60]. Using this device, it was observed that addition of varying levels of the inflammatory cytokine TNF-α caused a monotonic increase in platelet adhesion to the vessel walls, accompanied by significant amounts of fibrin. Modified versions of parallel plate flow chambers engraved in polycarbonate have also been used, utilizing micro-spotting of agonists and protein surfaces for platelet function testing, and temperature control modules for physiological temperatures[20,61]. Flow chambers incorporating stenoses such as that by Van Rooij et al[62]. have also been to study high shear platelet aggregation.

Devices specifically for hemostasis modeling have also been reported, including an “H” shaped PDMS device by Schoeman et al[63]. Whole blood is perfused through one of the vertical channels with buffer in the other. Collagen and TF coated to the crossbar of the “H” provide a thrombogenic surface on which whole blood can clot when the pressure in the wash buffer channel is reduced to induce transport from the blood channel to the ‘extravascular’ channel. Platelet inhibitors, omission of either collagen or tissue factor, and factor VIII inhibitors were all found to prolong closure time. In another bleeding model, Sakurai et al. utilized a HUVEC vascularized PDMS device, with the addition of a pneumatic microvalve to incorporate a extravascular bleeding into the assay[64]. Using this device, it was shown that $\alpha_{2b}\beta_3$ blocking agent eptifibatide did not impact wound closure time, but did reduce platelet density via impaired contraction, and also recapitulated increased bleeding in Hemophilia A blood when compared with healthy. More recently, Lakshmanan et al. developed a similar device for potential assessment of bleeding in COVID-19 patients[65]. Using a “T” shaped orientation, a PDMS device was designed with vertical pillars in the cross-section of the “bleeding” channel, which is functionalized with fibrillar collagen, where the pillars are used to model disturbed endothelium owing to inflammation. Hemostatic plugs were found to form in the bleeding channel, accompanied by reduction in the fluid velocity in the bleeding channel.

Several paper-based microfluidic devices have also been utilized to for coagulation screening. Owing generally to its low cost, hydrophilicity, and ubiquity, paper is a commonly used substrate for microfluidic assays[66]. A lateral flow assay (LFA) device designed by Li et al.[67] utilizes a cellulose membrane to separate red blood cells from citrated whole blood. The distance of RBC penetration into the membrane enables a metric which can be related to clotting time. Another device by Sweeney et al.[68] utilizes wax treated nitrocellulose paper preloaded with either heparin or protamine, and observed a similar clotting time dependent penetration of red blood cells, where low lengths were detected optically.

Microfluidic devices using non-optical detection methods have been developed recently as well. Roka-moiia et al. demonstrated a microfluidic device with a magnetic stir bar used to detect electrical impedance[69]. Using a cylindrical well agitated by the stir bar and 2 electrodes, impedance was monitored and found to increase on addition of various agonists such as ADP and collagen. A similar detection method has been demonstrated by Maji et al.[70] using dielectric spectroscopy in a static assay to detect changes in the permittivity of whole blood as clotting occurs in a PMMA device. Shifts the timing of a peak in the permittivity were observed for changes in temperature, calcium concentration, and additions of thrombin or antithrombin. This technology has been developed further into a point-of-care product: ClotChip, by XaTek. Other detection technologies have been demonstrated such as IR spectroscopy, by Ansell et al.[71] in a product produced by Perosphere Technologies.

In a recent study, Rossi and Diamond[49] demonstrated the creation of a single use fully assembled, disposable chip that had 6-month storage stability at 4C under dry conditions. The injection-molded chip featured a single luer lock connect for priming by a 1-mL syringe, wells with standard 96-well spatial separation (allowing for rapid multichannel pipetting of reagents and chip loading) and a single luer lock connect to drive fluid motion by connection to a constant pressure controlled vacuum pump. The chip had 8 individual channels for blood flow across a 250-micron wide strip of patterned surface of fibrillar type 1 collagen and lipidated TF. Use of fluorescent tags for fibrin and platelets and 2-color imaging with a small portable epifluorescent microscope allowed monitoring of 8 individual clotting events. This device has been demonstrated to have sensitivity for detection of Factor Xa inhibitors such as apixaban, rivaroxaban and dabigatran via monitoring reductions in fibrin fluorescence signal. In another device designed for drug detection, Al-aqbi et al[72] have demonstrated separation and concentration of aminoglycoside drugs from whole blood using electrophoresis in an PMMA device. Nanojunctions are generated in the device by dielectric breakdown of the, allowing separation of drugs and blood components by size and mobility. Drug detection for potential point of care monitoring has also been demonstrated using other technologies[50,51,71].

Priming with a bovine serum albumin solution (BSA) (Fig. 1A) passivated the polymer surface, preventing undesired contact pathway activation in CTI-treated blood and preventing air bubbles during blood perfusion (Fig. 1B). Platelets rapidly adhere and activate on the fibrillar collagen while thrombin and fibrin are generated specifically at the location of the patterned collagen/TF that crosses each flow channel. The intrachip uniformity of flow and clotting in the 8 replicates was 10 % CV (Fig. 1C). Across many healthy adult donors (n = 10) the interdonor variability in coagulation was 30% CV for platelet deposition and 22% CV for fibrin deposition. Dynamic signals are rapidly obtained during the experiment. For example, the direct oral anticoagulant (DOAC) apixaban which is a potent Factor Xa inhibitor provided a dose-dependent inhibition of fibrin formation (Fig. 1D) allowing for the calculation of an IC50 = 120 nM for fibrin formation under flow conditions (Fig. 1E). Similar results were obtained for the Factor Xa DOAC rivaroxaban (IC50 = 120 nM) and the thrombin DOAC dabigatran (IC50 = 60 nM). Interestingly, the platelet deposition on the collagen is not particularly sensitive to the presence of DOAC until concentrations were greater than about 200 nM. In an important clinical application of rapid DOAC detection in the context of patients presenting with severe bleeding, trauma, or

emergency surgery, microfluidic testing can provide relevant information about DOAC level and the use of a DOAC reversal agent. In Fig. 1F, a level of 200 nM apixaban in whole blood was strongly reversed by the reversal agent andexanet alpha, which is a Gla-domain deficient/active-site mutant of FXa used to bind apixaban or rivaroxaban.

CONCLUSIONS

Many investigators have advanced the fields of vascular hemodynamics, cellular biorheology, adhesion dynamics, platelet signaling, von Willebrand factor (VWF) mechanobiology, and coagulation reaction network analysis. This interplay of fundamentalresearch using clinical samples continues to shed light on mechanisms of pathology and provides translational impact for the patient. Opportunities exist to define drug mechanism of action and drug potency using Lab-Chip tools. Clearly, microfluidics have proven to be a highly versatile tool to phenotype diverse aspects of blood function. While this review focused on thrombosis and hemostasis, lab-chip technologies will also impact other blood disorders as diverse as sickle cell anemia, inflammatory syndromes, COVID, or cancer. The technology for blood clotting under flow is beginning to reach the clinic with simple to use devices that minimize sample volume, sample processing, and provide faster quantitative readouts for clinical decision making.

ACKNOWLEDGMENTS

This work was supported by NIH grants R01-HL-103419 and U01-HL-131053 to SLD.

REFERENCES

1. Farndale RW, Sixma JJ, Barnes MJ and de Groot PG, Journal of Thrombosis and Haemostasis, 2004, 2, 561–573. [PubMed: 15102010]
2. Gemmell CH, Turitto VT and Nemerson Y, Blood, 1988, 72, 1404–1406. [PubMed: 3262388]
3. Sakariassen KS, Turitto VT and Baumgartner HR, Journal of Thrombosis and Haemostasis, 2004, 2, 1681–1690. [PubMed: 15456474]
4. Song H, Li HW, Munson MS, Ha TGV and Ismagilov RF, Analytical Chemistry, 2006, 78, 4839–4849. [PubMed: 16841902]
5. Neeves KB, Maloney SF, Fong KP, Schmaier AA, Kahn ML, Brass LF and Diamond SL, Journal of Thrombosis and Haemostasis, 2008, 6, 2193–2201. [PubMed: 18983510]
6. Colace T. v., Muthard RW and Diamond SL, Arteriosclerosis, Thrombosis, and Vascular Biology, 2012, 32, 1466–1476.
7. Li M, Hotaling NA, Ku DN and Forest CR, PLoS ONE, , DOI:10.1371/journal.pone.0082493.
8. Herbig BA and Diamond SL, Journal of Thrombosis and Haemostasis, 2015, 13, 1699–1708. [PubMed: 26178390]
9. Lehmann M, Schoeman RM, Krohl PJ, Wallbank AM, Samaniuk JR, Jandrot-Perrus M and Neeves KB, Arteriosclerosis, Thrombosis, and Vascular Biology, 2018, 38, 1052–1062.
10. Maloney SF, Brass LF and Diamond SL, Integrative Biology, 2010, 2, 183–192. [PubMed: 20473398]
11. Zhu S and Diamond SL, Thrombosis Research, 2012, 134, 1335–1343.
12. White-Adams TC, Berny MA, Patel IA, Tucker EI, Gailani D, Gruber A and McCarty OJT, Journal of Thrombosis and Haemostasis, 2010, 8, 1295–1301. [PubMed: 20796202]
13. Zhu S, Herbig BA, Yu X, Chen J and Diamond SL, Frontiers in Medicine, 2018, 5, 1–8. [PubMed: 29410956]
14. Springer TA, Journal of Thrombosis and Haemostasis, 2011, 9, 130–143. [PubMed: 21781248]

15. Brass LF and Diamond SL, Journal of Thrombosis and Haemostasis, 2016, 14, 906–917. [PubMed: 26848552]
16. Liu ZL, Ku DN and Aidun CK, Journal of Biomechanics, , DOI:10.1016/j.jbiomech.2021.110349.
17. Colace T. v., Tormoen GW, McCarty OJT and Diamond SL, Annual Review of Biomedical Engineering, 2013, 15, 283–303.
18. Fogelson AL and Neeves KB, Annual Reviews in Fluid Mechanics, 2015, 47, 377–403.
19. Okorie UM and Diamond SL, Biophysical Journal, 2006, 91, 3474–3481. [PubMed: 16905604]
20. de Witt SM, Swieringa F, Cavill R, Lamers MME, van Kruchten R, Mastenbroek T, Baaten C, Coort S, Pugh N, Schulz A, Scharrer I, Jurk K, Zieger B, Clemetson KJ, Farndale RW, Heemskerk JWM and Cosemans JMEM, Nature Communications, , DOI:10.1038/ncomms5257.
21. Zhu S, Tomaiuolo M and Diamond SL, Integrative Biology (United Kingdom), 2016, 8, 813–820.
22. Zhang Y and Diamond SL, Thrombosis Research, 2020, 192, 141–151. [PubMed: 32480168]
23. Li R, Grosser T and Diamond SL, Platelets, 2017, 28, 457–462. [PubMed: 28102731]
24. Sabrkhany S, Griffioen AW, Pineda S, Sanders L, Mattheij N, van Geffen JP, Aarts MJ, Heemskerk JWM, oude Egbrink MGA and Kuijpers MJE, European Journal of Cancer, 2016, 66, 47–54. [PubMed: 27525572]
25. DeCortin ME, Brass LF and Diamond SL, Research and Practice in Thrombosis and Haemostasis, 2020, 4, 1158–1166. [PubMed: 33134782]
26. Muthard RW and Diamond SL, Lab on a Chip, 2013, 13, 1883–1891. [PubMed: 23549358]
27. Muthard RW and Diamond SL, Arteriosclerosis, Thrombosis, and Vascular Biology, 2012, 32, 2938–2945.
28. Stalker TJ, Welsh JD and Brass LF, Current Opinion in Hematology, 2014, 21, 410–417. [PubMed: 25023471]
29. DeCortin ME, Brass LF and Diamond SL, Research and Practice in Thrombosis and Haemostasis, 2020, 4, 1158–1166. [PubMed: 33134782]
30. Stalker TJ, Traxler EA, Wu J, Wannemacher KM, Cermignano SL, Voronov R, Diamond SL and Brass LF, Blood, 2013, 121, 1875–1885. [PubMed: 23303817]
31. Welsh JD, Poventud-Fuentes I, Sampietro S, Diamond SL, Stalker TJ and Brass LF, Journal of Thrombosis and Haemostasis, 2017, 15, 526–537. [PubMed: 27992950]
32. Trigani KT and Diamond SL, Thrombosis and Haemostasis, 2021, 121, 46–57. [PubMed: 32961573]
33. Chen Z, Lu J, Zhang C, Hsia I, Yu X, Marecki L, Marecki E, Asmani M, Jain S, Neelamegham S and Zhao R, Nature Communications, , DOI:10.1038/s41467-019-10067-6.
34. Denis C. v. and Wagner DD, Cellular and Molecular Life Sciences, 1999, 56, 977–990. [PubMed: 11212329]
35. Bark DL and Ku DN, Journal of Biomechanics, 2010, 43, 2970–2977. [PubMed: 20728892]
36. Kragh T, Napoleone M, Fallah MA, Gritsch H, Schneider MF and Reininger AJ, Thrombosis Research, 2014, 133, 1079–1087. [PubMed: 24681085]
37. Tsiklidis EJ, Sinno T and Diamond SL, American Journal of Physiology - Heart and Circulatory Physiology, 2019, 317, H73–H86. [PubMed: 30978134]
38. Yu X, Tan J and Diamond SL, Journal of Thrombosis and Haemostasis, 2018, 16, 316–329. [PubMed: 29156107]
39. Yu X and Diamond SL, Thrombosis and Haemostasis, 2019, 119, 586–593. [PubMed: 30722079]
40. Colace T. v., Muthard RW and Diamond SL, Arteriosclerosis, Thrombosis, and Vascular Biology, 2012, 32, 1466–1476.
41. Tovar-Lopez FJ, Rosengarten G, Westein E, Khoshmanesh K, Jackson SP, Mitchell A and Nesbitt WS, Lab on a Chip, 2010, 10, 291–302. [PubMed: 20091000]
42. van Rooij BJM, Závodszky G, Hoekstra AG and Ku DN, Scientific Reports, 2020, 10, 1–11. [PubMed: 31913322]
43. Zhu S, Travers RJ, Morrissey JH and Diamond SL, Blood, 2015, 126, 1494–1502. [PubMed: 26136249]
44. Zhu S, Lu Y, Sinno T and Diamond SL, Journal of Biological Chemistry, 2016, 291, 23027–23035.

45. Nergiz-Unal R, Cosemans JMEM, Feijge MAH, van der Meijden PEJ, Storey RF, van Giezen JJJ, oude Egbrink MGA, Heemskerk JWM and Kuijpers MJE, PLoS ONE, 2010, 5, 1–13.
46. Li R, Fries S, Li X, Grosser T and Diamond SL, Clinical Chemistry, 2012, 59, 1195–1204.
47. Colace T. v. and Diamond SL, Arteriosclerosis, Thrombosis, and Vascular Biology, 2013, 33, 105–113.
48. Flamm MH, Colace T. v., Chatterjee MS, Jing H, Zhou S, Jaeger D, Brass LF, Sinno T and Diamond SL, Blood, 2012, 120, 190–198. [PubMed: 22517902]
49. Rossi JM and Diamond SL, Biomicrofluidics, , DOI:10.1063/5.0023312.
50. Maji D, Opneja A, Suster MA, Bane KL, Wilson BM, Mohseni P and Stavrou EX, Thrombosis and Haemostasis, 2021, 121, 58–69. [PubMed: 32877954]
51. Frydman GH, Ellett F, van Cott EM, Hayden D, Majmudar M, Vanderburg CR, Dalzell H, Padmanabhan DL, Davis N, Jorgensen J, Toner M, Fox JG and Tompkins RG, Critical Care Explorations, 2019, 1, e0024. [PubMed: 32166266]
52. Herbig BA, Yu X and Diamond SL, Biomicrofluidics, 2018, 12, 1–10.
53. Loyau S, Ho-Tin-noé B, Bourrienne MC, Boulaftali Y and Jandrot-Perrus M, Arteriosclerosis, Thrombosis, and Vascular Biology, 2018, 38, 2626–2637.
54. Yu X and Diamond SL, Thrombosis and Haemostasis, 2019, 119, 586–593. [PubMed: 30722079]
55. Ardillon L, Ternisien C, Fouassier M, Sigaud M, Lefrançois A, Pacault M, Ribeyrol O, Fressinaud E, Boisseau P and Trossaërt M, Haemophilia, 2015, 21, 646–652. [PubMed: 25753785]
56. Levy JH, Szlam F, Wolberg AS and Winkler A, Clinics in Laboratory Medicine, 2014, 34, 453–477. [PubMed: 25168937]
57. Wool GD, American Journal of Clinical Pathology, 2019, 151, 1–17. [PubMed: 30215666]
58. Dillinger JG, Si Moussi T, Berge N, Bal Dit Sollier C, Henry P and Drouet L, Thrombosis Research, 2016, 140, 66–72. [PubMed: 26901852]
59. Jain A, Graveline A, Waterhouse A, Vernet A, Flaumenhaft R and Ingber DE, Nature Communications, 2016, 7, 1–10.
60. Jain A, van der Meer AD, Papa AL, Barrile R, Lai A, Schlechter BL, Otieno MA, Louden CS, Hamilton GA, Michelson AD, Frelinger AL and Ingber DE, Biomedical Microdevices, 2016, 18, 1–7. [PubMed: 26660457]
61. Herfs L, Swieringa F, Jooss N, Kozlowski M, Heubel-Monen F, van Oerle R, Machiels P, Henskens YMC and Heemskerk JWM, Thrombosis Journal, 2021, 203, 46–56.
62. van Rooij BJM, Závodszky G, Hoekstra AG and Ku DN, Interface Focus, 2021, 11, 1–11.
63. Schoeman RM, Rana K, Danes N, Lehmann M, di Paola JA, Fogelson AL, Leiderman K and Neeves KB, Cellular and Molecular Bioengineering, 2017, 10, 3–15. [PubMed: 28529666]
64. Sakurai Y, Hardy ET, Ahn B, Tran R, Fay ME, Ciciliano JC, Mannino RG, Myers DR, Qiu Y, Carden MA, Baldwin WH, Meeks SL, Gilbert GE, Jobe SM and Lam WA, Nature Communications, 2018, 9, 1–9.
65. Lakshmanan HHS, Pore AA, Kohs TCL, Yazar F, Thompson RM, Jurney PL, Maddala J, Olson SR, Shatzel JJ, Vanapalli SA and McCarty OJT, Cellular and Molecular Bioengineering, 2020, 13, 331–339.
66. Sachdeva S, Davis RW and Saha AK, Frontiers in Bioengineering and Biotechnology, 2021, 8, 1–14.
67. Li H, Han D, Pauletti GM and Steckl AJ, Lab on a Chip, 2014, 14, 4035–4041. [PubMed: 25144164]
68. Sweeney R, Nguyen V, Alouidor B, Budiman E, Wong R and Yoon J-Y, IEEE Sensors Journal, 2019, 13, 4743–4751.
69. Roka-Moiia Y, Bozzi S, Ferrari C, Mantica G, Dimasi A, Rasponi M, Santoleri A, Scavone M, Consolo F, Cattaneo M, Slepian MJ and Redaelli A, International Journal of Molecular Sciences, , DOI:10.3390/ijms21041174.
70. Maji D, Suster MA, Kucukal E, Sekhon U, sen Gupta A, Gurkan U and Stavrou E, IEEE Trans Biomed Circuits Syst, 2017, 11, 1459–1469. [PubMed: 28920906]
71. Ansell J, Zappe S, Jiang X, Chen L, Steiner S, Laulicht B and Bakhru S, Seminars in Thrombosis and Hemostasis, 2019, 45, 259–263. [PubMed: 30566966]

72. Al-Aqbi ZT, Yap YC, Li F and Breadmore MC, Biosensors, , DOI:10.3390/bios9010019.

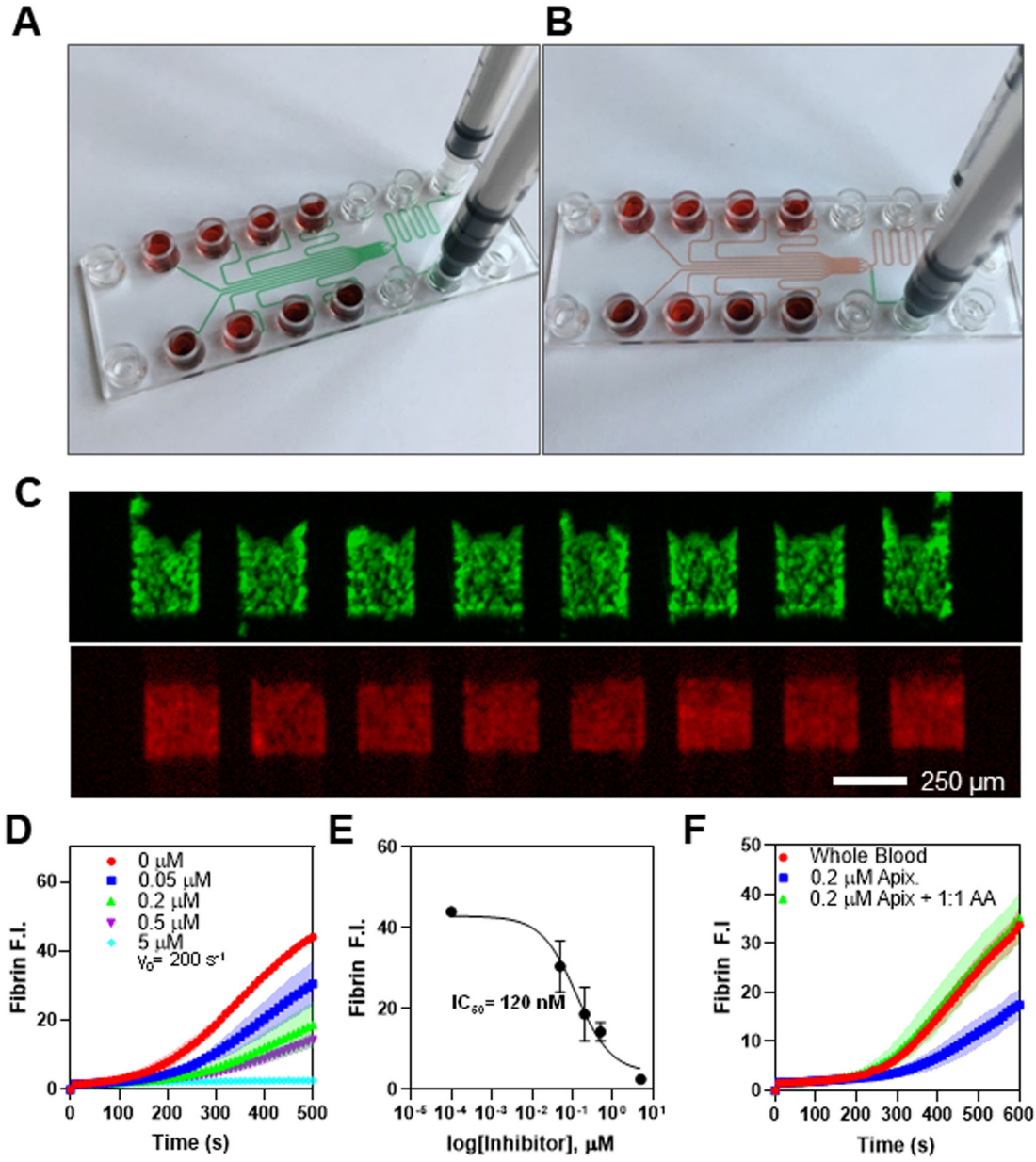

Fig. 1.

(A) Visual demonstration of device priming, where priming buffer (green) injected in the priming inlet arrives at each inlet port and the outlet port simultaneously. (B) Blood added to the inlet wells displaces priming fluid when negative pressure is applied at the outlet. (C) Fluorescence images for AF488-conjugated anti-CD61 (green) and AF594-conjugated human fibrinogen (red) for clots formed under flow. (D) Dose response in fibrin fluorescence intensity for addition of apixaban to whole blood ex vivo, and represented as an IC50 curve (E). (F) Fibrin FI for whole blood perfused as collected, with the addition of 200 nM apixaban ex vivo, and with both apixaban and an equimolar ratio of Andexanet Alfa reversal agent, where reversal agent restores the FI to uninhibited levels. All data obtained with human blood from consenting adults under IRB approval (University of Pennsylvania).

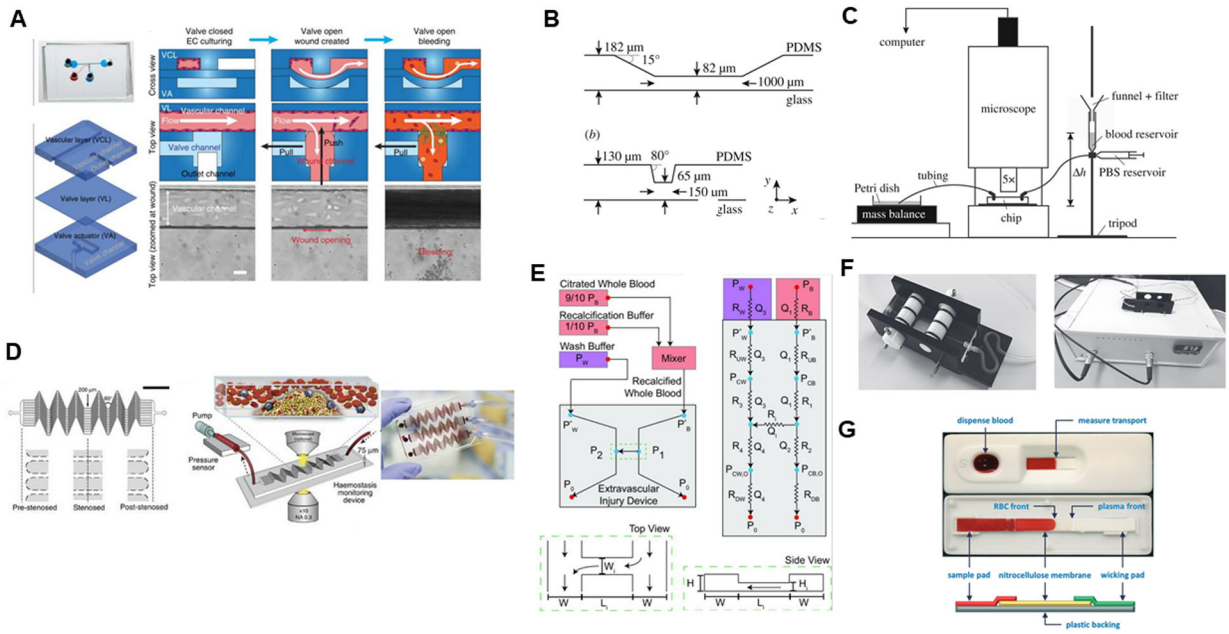

Fig. 2.

(A) Endothelialized PDMS microfluidic device with pneumatic valve to model vascular injury and subsequent bleeding, by Sakuri et al, reproduced from Figure 1C in original publication[64], licensed under CC-BY 4.0. (B) Stenotic flow chamber and (C) experimental apparatus to image stenotic region under flow by van Rooij et al, reproduced from Fig 1 in original publication[62] licensed under CC-BY 4.0. (D) Hemostasis monitoring device, blood is perfused through device with an inline pressure sensor which detects clotting time by Jain et al., reproduced from Figure 1A–C in original publication[59] licensed under CC-BY 4.0. (E) Bleeding model microfluidic device, where whole blood is perfused through one channel, and buffer through the other at different flow rates to induce pressure drop across device. Reproduced with permission[63] from the BMES. (F) Maastricht flow chamber with temperature control module, by Herfs et al, reproduced from Figure 1 in original publication[61] licensed under CC-BY 4.0.(G) Nitrocellulose paper microfluidic device where RBC front extension length into paper is used to detect coagulation, by Li et al, reproduced from Figure 2 in original publication[67], with permission from the Royal Society of Chemistry.

Table 1

Common drugs utilized to inhibit either platelets aggregation or coagulation, along with their corresponding physiological target and efficacious dose.

AGENT	TARGET	Microfluidic Potency	Comment	Ref.
anti-Platelet				
ASA	COX-1 synthesis of thromboxane	IC50 =~ 15μM (venous)	Effects seen > 150 sec of clotting	7,46
MRS-2179	P2Y1 (prevents ADP binding)	0.218 μM IC50	slows clot growth of shell	10,25
2-Me-SAMP	P2Y12 (prevents ADP binding)	2.2 μM IC50	slows clot growth of shell	10,23
dasatinib	src/syk (mitigates GPVI signaling)	Platelets blocked at 1 μM	minimal platelet coverage of collagen	23
GR-144053	blocks fibrinogen binding to a2bb3	26 nM IC50	platelet monolayer on collagen	47
apyrase	degrades ADP, ATP	Not active at 1 U/mL	Inactive or stimulatory under flow	10
iloprost	IP receptor (prostacyclin receptor)	>80% reduction at 1 μM	reduced platelet deposition	48
anti-Coagulant				
apixaban	Factor Xa	120 nM IC50	Activity determined by fibrin signal	49–51
rivoraxaban	Factor Xa	120 nM IC50	Activity determined by fibrin signal	49–51
dabigatran	thrombin	60 nM IC50	Activity determined by fibrin signal	49,50
PPACK	thrombin, FXIIa	Complete inhibition 100 μM	Useful for platelet function studies	10
CTI	FXIIa	Full inhibition of contact activation at 40 μg/mL	Useful for blood collection for extrinsic pathway studies	10,52
14E11, O1A6	FXIa	fibrin blocked at 20 μg/mL	Less potent if TF present	43
GPRP	Fibrin polymerization	Polymerization inhibition at 5 mM		40
PPXbd	platelet polyphosphate	250 μg/mL	fibrin reduced at > 7 min	43
Andexanet Alfa	reversal agent	Restoration of fibrin at equimolar with Xa inhibitor		49
tPA	fibrin	10–50 nM to dissolve fibrin	Rapid lysis of fibrin	53,54